Layer-by-Layer-Assembled Microfiltration Membranes for Biomolecule Immobilization and Enzymatic Catalysis

V. Smuleac,[†,‡] D. A. Butterfield,[‡,§] and D. Bhattacharyya*[,†,‡]

Departments of Chemical and Materials Engineering and of Chemistry and Center of Membrane Sciences, University of Kentucky, Lexington, Kentucky 40506

Received April 25, 2006. In Final Form: September 5, 2006

Multilayer assemblies of polyelectrolytes, for protein immobilization, have been created within the membrane pore domain. This approach was taken for two reasons: (1) the high internal membrane area can potentially increase the amount of immobilized protein, and (2) the use of convective flow allows uniform assembly of layers and eliminates diffusional limitations after immobilization. To build a stable assembly, the first polyelectrolyte layer was covalently attached to the membrane surface and inside the pore walls. Either poly(L-glutamic acid) (PLGA) or poly(L-lysine) (PLL) was used in this step. Subsequent deposition occurs by multiple electrostatic interactions between the adsorbing polyelectrolyte [poly(allylamine) hydrochloride (PAH) or poly(styrenesulfonate) (PSS)] and the oppositely charged layer. Three-layer membranes were created: PLL−PSS−PAH or PLGA−PAH−PSS, for an overall positive or negative charge, respectively. The overall charge on both the protein and membrane plays a substantial role in immobilization. When the protein and the membrane are oppositely charged, the amount immobilized and the stability within the polyelectrolyte assembly are significantly higher than for the case when both have similar charges. After protein incorporation in the multilayer assembly, the active site accessibility was comparable to that obtained in the homogeneous phase. This was tested by affinity interaction (avidin−biotin) and by carrying out two reactions (catalyzed by glucose oxidase and alkaline phosphatase). Besides simplicity and versatility, the ease of enzyme regeneration constitutes an additional benefit of this approach.

Introduction

The layer-by-layer (LbL) assembly technique, most commonly conducted by intercalation of positive and negative polyelectrolytes,[1,2] is a powerful, versatile, and simple method for assembling supramolecular structures. These structures exhibit negative and positive charges, which allow for incorporation of a variety of materials: dyes, crystals, particles, or biomolecules. For this reason, the LbL assembly technique has found applications in a multitude of areas: nonlinear optical materials formation,[3,4] patterning,[5] separations,[6−9] biosensing,[10,11] biocatalysis, and others. For biocatalysis in particular, since enzymes are multiply charged molecules, electrostatic adsorption seems to be one of the simplest ways to perform the immobilization. Other common methods of enzyme immobilization, such as physical adsorption,[12] encapsulation,[13] or random covalent attachment,[14,15] have disadvantages in terms of stability and low active site accessibility/activity. Site-directed immobilization[16−19] requires complex steps but does provide highly enhanced activity.

Thus, a number of papers showed successful enzyme immobilization by electrostatic encapsulation[20,21] or adsorption on polyelectrolyte-modified slides,[22] resins,[23] films,[24] particles,[25−27] or membranes.[28−30] Membranes have distinct advantages over other supports, as the use of convective flow eliminates substrate diffusion problems, and the product is transported away from the enzyme active site during operation. This is particularly important when the product acts as an inhibitor. Also membranes have a high surface area, which offers a potentially higher protein/enzyme

* To whom correspondence should be addressed. Phone: (859) 257-2794. Fax: (859) 323-1929. E-mail: db@engr.uky.edu.

† Department of Chemical and Materials Engineering.

‡ Center of Membrane Sciences.

§ Department of Chemistry.

(1) Decher, G.; Hong, G. D.; Schmitt, J. J. *Thin Solid Films* **1992**, *210*, 831−835.

(2) Decher, G. *Science* **1997**, *277*, 1232−1237.

(3) Lvov, Y.; Yamada, S.; Kunitake, T. J. *Thin Solid Films* **1997**, *300*, 107−112.

(4) Shimazaki, Y.; Ito, S.; Tsutsumi, N. *Langmuir* **2000**, 16, 9478−9482.

(5) Zheng, H.; Lee, I.; Rubner, M. F.; Hammond, P. T. *Adv. Mater.* **2002**, *14*, 569−572.

(6) Malaisami, R.; Bruening, M. L. *Langmuir* **2005**, *21*, 10587−10592.

(7) Wanqin, J.; Toutianoush, A.; Thieke, B. *Langmuir* **2003**, *19*, 2550−2553.

(8) Kraseman, L.; Thieke, B. *J. Membr. Sci.* **1998**, *150*, 23−30.

(9) Liu, X.; Bruening, M. L. *Chem. Mater.* **2004**, *16*, 351−357.

(10) Forzani, S. E.; Solis, V. M. *Anal. Chem.* **2000**, *72*, 5300−5307.

(11) Wu, Z.; Guan, L.; Shen, G.; Yu, R. *Analyst* **2002**, 391−395.

(12) Koga, J.; Yamaguchi, K.; Gondo, S. *Biotechnol. Bioeng.* **1984**, *26*, 100−103

(13) Bhatia, R. B.; Brinker, J. C.; Gupta, A. K.; Singh A. K. *Chem. Mater.* **2000**, *12*, 2434−2441.

(14) Li, Z. F.; Kang, E. T.; Neoh, K. G.; Tan, K. L. *Biomaterials* **1998**, *19*, 45−53.

(15) Godjevargova, T.; Konsulov, V.; Dimov, A.; Vasileva, N. *J. Membr. Sci.* **2000**, *172*, 279−285.

(16) Vishvanath, S. K.; Watson, C. R.; Huang, W.; Bachas, L. G.; Bhattacharyya, D. *J. Chem. Technol. Biotechnol.* **1997**, *68*, 294−302.

(17) Ganapathi-Desai, S.; Butterfield, D. A.; Bhattacharyya, D. *Biotechnol. Prog.* **1998**, *14*, 865−873.

(18) Butterfield, D. A.; Bhattacharyya, D.; Daunert, S.; Bachas, L. G. *J. Membr. Sci.* **2001**, *181*, 29−37.

(19) Amounas, M.; Innocent, C.; Cosnier, S.; Seta, P. *J. Membr. Sci.* **2000**, *176*, 169−176.

(20) Wang, Y.; Caruso, F. *Chem. Mater.* **2005**, *17*, 953−961.

(21) Zhu, H.; McShane, J. *Langmuir* **2005**, *21*, 424−430.

(22) Constantine, C. A.; Mello, C. V.; Dupont, A.; Cao, X.; Santos, D.; Oliveira, O. N.; Strixino, F. T.; Pereira, E. C.; Cheng, T. C.; Defrank, J. J.; Leblanc, R. M. *J. Am. Chem. Soc.* **2003**, *125*, 1805−1809.

(23) Fuentes, M.; Maquiese, J. V.; Pessela, B. C. C.; Abian, O.; Fernandez-Lafuente, R.; Mateo, C.; Guisan, J. M. *Biotechnol. Prog.* **2004**, *20*, 284−288.

(24) Lvov, Y.; Ariga, K.; Ichinose, I.; Kunitake, T. *J. Am. Chem. Soc.* **1995**, *117*, 6117−6123.

(25) Khopade, A. J.; Caruso, F. *Langmuir* **2003**, *19*, 6219−6225.

(26) Haupt, B.; Neumann, Th.; Wittemann, A.; Ballauff, M. *Biomacromolecules* **2005**, *6*, 948−955.

(27) Lee, Y.; Stanish, I.; Rastogi, V.; Cheng, T. C.; Singh, A. *Langmuir* **2003**, *19*, 1330−1336.

(28) Nguyen, Q. T.; Ping, Z.; Nguyen, T.; Rigal, P. *J. Membr. Sci.* **2003**, *213*, 85−95.

(29) Wang, Y.; Caruso, F. *Adv. Funct. Mater.* **2004**, *14*, 1012−1018.

(30) Yu, A.; Liang, Z.; Caruso, F. *Chem. Mater.* **2005**, *17*, 171−175.

10.1021/la061124d CCC: $33.50
Published on Web 10/18/2006 PAGE EST: 7

loading. For practical applications this is important, as these properties increase the reaction throughput and protein recovery.

Traditional layer-by-layer assemblies are synthesized using alternate polyanion/polycation deposition on the membrane external surface, and thin films are obtained, typically on the order of tens to hundreds of nanometers. However, due to the small external membrane surface area, only a low amount of enzyme can be immobilized. Another alternative is to grow the multilayer assemblies inside the membrane pores, as the internal membrane area is much higher. The polyelectrolytes can be transported through the membrane under convective conditions, and the film is grown perpendicular to the direction of solvent flux until the desired pore coverage is achieved.

In one of our recent papers,[31] this approach was implemented to create pore-assembled charged multilayers for nanofiltration-type separations. In the present work, we extend the fabrication of the charged multilayer assemblies inside the membrane pores to subsequent electrostatic incorporation of biomolecules. The major goal of this study is to evaluate whether this multilayer structure can be used effectively to immobilize biomolecules with minimum loss of activity while achieving high loading. The active site accessibility upon biomolecule immobilization was tested on the basis of affinity interactions (using the avidin−biotin model) and two enzymatic reactions (catalyzed by glucose oxidase and alkaline phosphatase). Ease of enzyme reusability is an important aspect of this multilayer technique.

Materials and Methods

Materials. Immunodyne ABC nylon membranes, with an average pore size of 450 nm, manufactured by Pall Corp. were used as a support for multilayer assembly. Poly(L-glutamic acid) (PLGA), MW 21500, poly(L-lysine) (PLL), MW 74900, bovine serum albumine (BSA), avidin, biotinylated amidobenzoic acid (BABA), glucose oxidase (GOx) from *Aspergillus niger*, lot no. 015K0799, alkaline phosphatase (AP) from *Escherichia coli*, lot no. 114K4155, and *p*-nitrophenyl phosphate were purchased from Sigma. Poly(styrenesulfonate) (PSS), MW 70000, poly(allylamine) hydrochloride (PAH), MW 70000, titanium(IV) oxysulfate, and *p*-nitrophenol were supplied through Aldrich. The protein assay kit was obtained from BioRad Laboratories. Hydrogen peroxide, sodium hydroxide, hydrochloric acid, and deionized ultrafiltered (DIUF) water were purchased from Fisher Scientific.

Multilayer Assembly Formation. The multilayer assembly was formed within the pore domain, under convective conditions.The first layer must be covalently attached to the pore wall, to ensure the stability of the entire structure. Subsequent deposition occurs by multiple electrostatic interactions between the adsorbing polyelectrolyte and the oppositely charged layer, already on the membrane. Immunodyne ABC nylon membranes (Figure 1), were prefunctionalized by the manufacturer with anhydride groups, thus being suitable for amine coupling. The structure of the polyelectrolytes used in the assembly formation is presented in Figure 2. Amine-terminated poly(amino acid)s were permeated through the membrane, yielding covalently anchored polymer chains. Thus, multilayer formation always begins with single-point covalent attachment of either negatively charged PLGA or positively charged PLL. In the case of PLGA, there is only one amino group per molecule, whereas for PLL there is an amino group in the α position with a pK_a of 9.1 and on the side chain (pK_a of 10.6).[32] The attachment of PLL was conducted at a pH of 9.4−9.6, which ensures that only the amino group in the α position is deprotonated, thus being the only one suitable for covalent coupling. The schematic of the PLGA−PAH−PSS assembly formation is presented in Figure 3. The PLL−PSS−PAH assembly was built in an analogous way. After completion of the three-layer structure, BSA, avidin, GOx, or AP was electrostatically immobilized. In addition to the three-layer assembly, a control experiment was performed, immobilizing a single layer (PLL) followed by GOx incorporation. This was done to check whether the assembly has a significant role in the amount immobilized or enzyme activity or a single layer would be sufficient.

Random (Covalent) Attachment. Random attachment of proteins was conducted by permeating the enzyme (GOx and AP, respectively) solutions through the membrane, at neutral pH. As mentioned before, the membranes were prefunctionalized with anhydride groups for amine coupling.

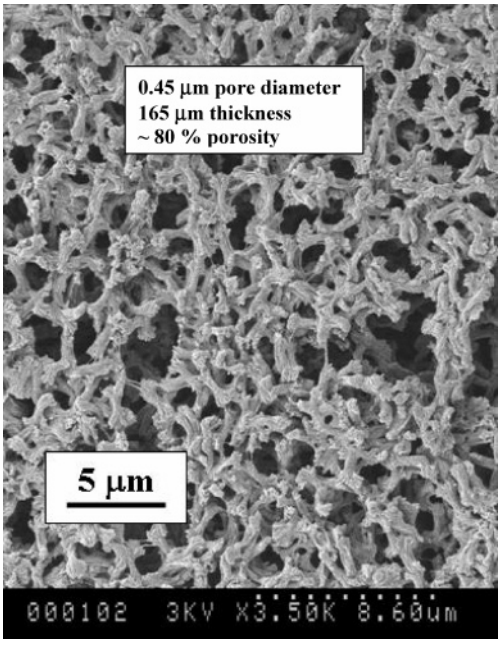

Figure 1. Scanning electron microscopy (SEM) image of the nylon-based microfiltration membrane surface.

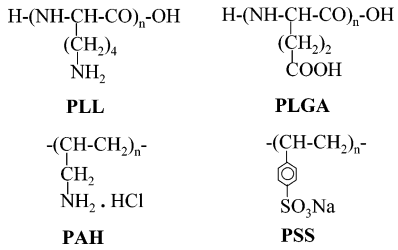

Figure 2. Schematics of the polyelectrolytes used in the multilayer assembly formation.

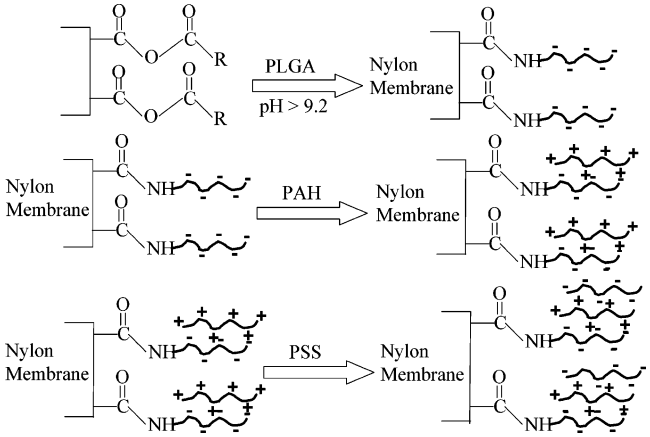

Figure 3. Nylon membrane functionalization to create the multilayer assembly with polyions by covalent attachment and electrostatic interactions.

(31) Hollman, A. M.; Bhattacharyya, D. *Langmuir* **2004**, *20*, 5418−5424.
(32) Voet, D.; Voet J. G.; Pratt, C. W. *Fundamentals of Biochemistry*; John Wiley & Sons: New York, 1999; p 81

Polyelectrolyte Quantification. The concentration of PLGA, PLL, and PAH in feed permeate solutions was estimated by total organic carbon (TOC) analysis, using a TOC-5000A Shimadzu analyzer. The amount of each polyelectrolyte immobilized on the membrane was determined from material balance. Three replicates were taken for each measurement, and the error was <3%. The concentration of PSS in the feed and permeate solutions was determined from the absorbance at 260 nm. In the concentration range from 40 to 300 mg/L, the standard deviation for three replicates was up to 5%, with a correlation coefficient of 0.998.

Protein Determination. The amount of protein in the feed and permeate solutions was determined using the Bradford protein assay procedure.[33] A calibration curve was carried out with a BSA standard solution. An acidic dye was added to the protein solution, and the absorbance of the dye−protein complex was measured at 595 nm, with a standard deviation for three measurements of <0.1%. The amount immobilized on the membrane can be estimated from material balance.

Accessibility of the Active Sites. Avidin (pI of 10.5) was immobilized at pH 6 on a three-layer (PLGA−PAH−PSS), negatively charged membrane, followed by permeation of BABA. The concentration of BABA in the feed and permeate solutions was determined from the absorbance at 264 nm. Overall material balance provided the amount of BABA immobilized on the membrane. In the linear range from 2 to 10 mg/L the standard deviation was less than 5%.

Kinetic Studies. Two enzymes, glucose oxidase and alkaline phosphatase, were tested in these studies. The experiments were carried out in homogeneous and heterogeneous (immobilized) modes. In the homogeneous phase, the experiments were carried out in a mixed batch reactor at room temperature. In the immobilized form the substrate solution was permeated through the membrane, mounted in a dead-end filtration cell, pressurized with air, for GOx, and nitrogen, in the case of AP. Typical operating fluxes ranged from 14×10^{-4} to 17×10^{-4} cm^3/(cm^2 s) at 1.7 bar. Product formation was monitored by taking permeate samples at regular intervals.

The enzyme glucose oxidase catalyzes the reaction

$$\text{glucose} + O_2 \rightarrow \text{gluconic acid} + H_2O_2$$

Hydrogen peroxide was analyzed using a well-established colorimetric method.[34] An acidified titanium(IV) oxysulfate solution was added, and the absorbance of the yellow-colored titanium−peroxo complex was measured at 407 nm. For the concentration range from 2 to 100 mg/L, the standard deviation was <0.5%. Gluconic acid was analyzed using an ion chromatography system (IES 2500). The amounts of each product, determined by the two methods mentioned above, were less than 5% from the 1:1 molar ratio. This is within the experimental error associated with gluconic acid determination.

Alkaline phosphatase catalyzes the reaction[16]

$$p\text{-nitrophenyl phosphate} \rightarrow p\text{-nitrophenol} + \text{phosphate}$$

The reaction was monitored by measuring *p*-nitrophenol absorbance at 410 nm. The standard deviation for three replicates, in the concentration range from 1.4 to 8.4 mg/L, was less than 0.5%.

For both enzymes, reactions were conducted at four different substrate concentrations: between 2.5 and 25 mM for glucose and from 0.05 to 0.5 mM for *p*-nitrophenyl phosphate. The method of initial rates and Lineweaver−Burk plots were used to determine the Michaelis−Menten kinetic parameters K_M and v_{max}.

Results and Discussion

Pore Assembly Formation and Characterization. Using membranes as a support, layer-by-layer assemblies are usually built by alternate polyanion/polycation deposition on the external surface, via a soaking mode. However, due to the small external membrane surface area, a low protein/enzyme density is obtained. A method of producing high surface area enzyme thin films on membrane supports was recently reported.[30] The polyelectrolyte layers were deposited inside membrane pores by coating. Only thin films (up to seven bilayers) could be constructed, as the pore blockage and diffusional limitations have a dramatic effect on the enzyme activity. In addition, the pore blockage, due to preferential polyelectrolyte adsorption on the external membrane surface and pore mouth, causes an improper coating on the entire pore length. To overcome diffusional limitations and to achieve a high protein loading, in this study, the polyelectrolyte multilayer is formed within the pore domain under convective conditions. The pore assemblies were created over the thickness of the membrane. A schematic of the two approaches, polyelectrolyte adsorption/pore assembly formation, with subsequent protein immobilization is presented in Figure 4.

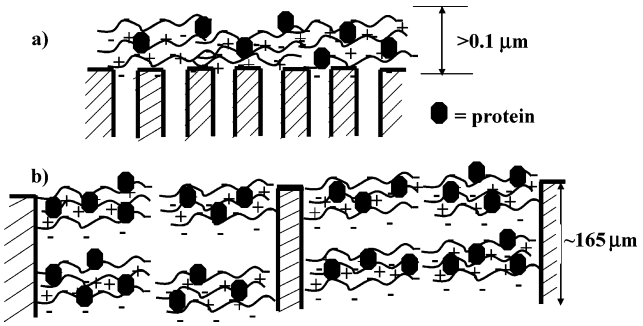

Figure 4. Protein immobilization in multilayer assemblies: (a) thin films of polyanion/polycation, obtained by alternate adsorption on the membrane surface, (b) pore-assembled multilayers.

Table 1. Polyelectrolyte Adsorption and the Net Charge for PLGA−PAH−PSS- and PLL−PSS−PAH-Modified Membranes

polyelectrolyte	amt adsorbed (mmol × 10^5)	net charge[a] (mmol × 10^3)
PLGA	9.7	−12.2
PLGA−PAH	2.5 (12.2)[b]	+18.5 (+6.3)[b]
PLGA−PAH−PSS	6.7 (18.9)[b]	−22.9 (−16.6)[b]
PLL	1.2	+6
PLL−PSS	2.5 (3.7)[b]	−8.5 (−2.5)[b]
PLL−PSS−PAH	1.7 (5.4)[b]	+13 (+10.5)[b]

[a] Calculated as amount adsorbed × number of repeat units. Number of repeat units: PLGA, 250; PAH, 749; PSS, 340; PLL, 486. [b] Cumulative.

Three-layered membranes, PLGA−PAH−PSS or PLL−PSS−PAH, were created. The amount of each polyelectrolyte adsorbed in the membrane is shown in Table 1. The polypeptide chain density (and thus the amount immobilized) is dependent on the chain length, due to steric and electrostatic effects. Steric effects lower the chain density because there is a closer packing for shorter chains (MW 21500 for PLGA) than for longer ones (MW 74900 for PLL), and the terminal amine group will be less accessible for the reaction with the aldehyde on the membrane surface. Electrostatic effects are due to the fact that the coupling reaction must be carried out at high pH (above 9.1, where the terminal amine group on PLL is deprotonated). At this pH the polypeptide is highly charged, which will cause repulsion between chains, lowering the chain density. Higher repulsion is expected between longer chains (more repeating units, all negatively charged). Thus, due to these steric and electrostatic effects, there is a lower chain density for PLL, as compared to PLGA. From the amount of the polyelectrolyte deposited and the number of repeat units, one can estimate the number of ionizable groups on each polyelectrolyte layer. Assuming stoichiometric interaction among the ionizable groups after adsorption of each layer, the

(33) Bradford, M. M. *Anal. Biochem.* **1976**, *72*, 248−254.
(34) Clapp, P. A.; Evans, D. F.; Sheriff, T. S. S. *Anal. Chim. Acta* **1989**, *218*, 331−334.

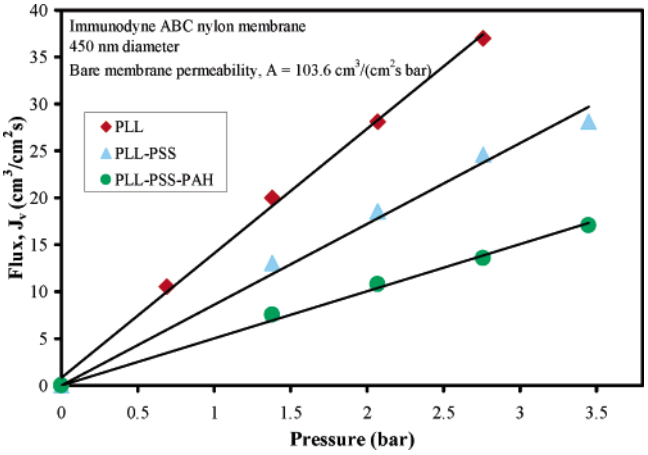

Figure 5. Pure water flux dependence on pressure for each polyelectrolyte multilayer adsorbed within the membrane.

Table 2. Estimated Polyelectrolyte Brush Thickness for Negatively and Positively Charged Membranes[a]

polyelectrolyte	thickness (nm)	polyelectrolyte	thickness (nm)
PLGA	55	PLL	91
PLGA−PAH	92	PLL−PSS	103
PLGA−PAH−PSS[b]	117	PLL−PSS−PAH[c]	119

[a] Nylon membrane, 33.2 cm^2 external area, 165 μm thickness. [b] PLGA-PAH−PSS, negatively charged membrane. [c] PLL-PSS−PAH, positively charged membrane.

net (overall) charge on PLGA−PAH−PSS is negative, 16.6 × 10^{-3} mmol, and on PLL−PSS−PAH the charge is positive, 10.5 × 10^{-3} mmol. For layer-by-layer assembly the overall charge corresponds to that of the outer layer.

Membrane permeability decreases as the number of layers of polyelectrolyte deposited on the membrane is increased. The flux after each layer deposition for the positively charged PLL−PSS−PAH membrane is presented in Figure 5. The linear relationship between the pure water flux (J_v) and applied pressure (ΔP) shows that the multilayer assembly is stable. A polyelectrolyte loss during operation would show an exponential increase of J_v vs ΔP.

The J_v vs ΔP plots can be used to estimate the equivalent pore diameter, d_c, applying Hagen−Poisseuille's law of capillary flow:

$$d_c = 2(8J_w\mu L/\pi N\Delta P)^{1/4} \quad (1)$$

where N, ΔP, μ, and L represent the number of pores, transmembrane pressure, viscosity of the flowing liquid, and membrane thickness, respectively. The estimation of the equivalent diameter was based on permeability changes for the bare and functionalized membrane. The water flux for the functionalized membrane is dependent on several parameters, such as the polyelectrolyte chain density, chain length, water flux, or pH.

Assuming no change in membrane thickness, $J_v/J_{v,0} = (d_p/d_{p,0})$,[4] where $J_{v,0}$ and $d_{p,0}$ are the pure water flux and the equivalent diameter for the bare membrane, respectively, and J_v and d_p are the pure water flux and the estimated equivalent diameter for the functionalized membrane after each step. The thickness of the polyelectrolyte brush, estimated as $(d_{p,0} - d_p)/2$, after the deposition of each layer within the pore is given in Table 2. Although the amount of PLL is less than that of PLGA, the brush thickness is lower for the latter one. This may be counterintuitive, but the length of PLL is 3 times larger, and as a consequence the membrane permeability is decreased more. Thus, assuming a cylindrical pore and uniform chain distribution, it can be estimated that after deposition of three layers on a positively charged membrane, more than 22% of the pore volume is not covered by polyelectrolyte chains. The importance of this will be discussed below.

Table 3. BSA (pI 4.7) Immobilization and Desorption from a Three-Layer Negatively Charged Membrane as a Function of pH

		amt desorbed after washing (mg)	
amt of BSA immobilized[a] (mg)	pH	DIUF water, pH 5.6	DIUF water, pH 9
2.5	3.5	0	0.05
0.09	6.2	0.05	0.04

[a] Three-layer PLGA−PAH−PSS, negatively charged membrane, 33.2 cm^2 external area, 165 μm thickness.

Protein Immobilization on a Charged Membrane. Protein immobilization on the polyelectrolyte-assembled membranes occurs via electrostatic interactions. As a consequence, it is important to establish the effect of the overall protein/membrane charge on immobilization The effect of membrane/protein charge on protein immobilization was tested by permeation of BSA (pI 4.8), through an overall negatively charged membrane (PLGA−PAH−PSS). The adsorption experiments on the same membrane were conducted at pH 3.5 and 6.3, at which BSA has an overall positive and negative charge, respectively.

There is a significant (25-fold) reduction in adsorption for the case when both BSA and the membrane have similar charges (Table 3). This is an order of magnitude higher compared to the results obtained when proteins are deposited on polyelectrolyte films,[35,36] under static conditions. It was suggested that when the protein and the polyelectrolyte film are oppositely charged, the adsorption occurs in an ordered fashion, proteins being oriented with their oppositely charged domain toward the film. The immobilized proteins form an oppositely charged surface for the adsorption of the next protein layer, so the adsorbed proteins form multilayers several times thicker than a monolayer. When both the protein and the film have the same charge, the adsorption occurs randomly and there is no net charge to promote a protein multilayer formation.

In this work, the protein adsorption is conducted in convective mode and the BSA molecules are mostly rejected from the multilayer-modified membrane at a pH of 6.3. Since proteins have both positive and negative domains, some proteins may be oriented with the oppositely charged domain toward the multilayer and also some PAH layers can emerge to the outer surface. As a consequence, a small amount of BSA is still adsorbed at pH 6.3. The desorption of the immobilized BSA for the two cases also occurs differently. For the case when the protein and the membrane have similar charges, there is a significant (56%) desorption even under mild washing conditions (DIUF water, at pH 5.6) and BSA is totally desorbed at pH 9, showing that the interaction with the multilayer is weak. When the protein and the modified membrane have opposite charges, no protein is desorbed at pH 5.6−8 and only a small fraction (2%) is released at pH 9.

To ensure system stability, and to increase the amount of immobilized protein, all subsequent investigations involved protein adsorption on an oppositely charged membrane only. Thus, avidin (pI 10.5) was immobilized on an overall negatively charged membrane over a pH range from 6 to 8. The two enzymes

(35) Ladam, G.; Gergely, C.; Senger, B.; Decher, G.; Voegel, J. C.; Schaaf, P.; Cuisinier, F. J. G. *Biomacromolecules* **2000**, *1*, 674−687.
(36) Ladam, G.;Schaaf, P.; Cuisinier, F. J. G.; Decher, G.; Voegel, J. C. *Langmuir* **2001**, *17*, 878−882

Table 4. Study of the Biomolecule Active Site Accessibility upon Immobilization on the Membrane Using the Avidin−Biotin Model

amt of avidin immobilized[a]				amt of BABA attached with avidin		max uptake possible[b]		
mg	mmol	BABA feed concn (mg/L)	pH	mg	mmol	mg	mmol	avidin site accessibility (%)
1.36	2.3×10^{-5}	13.5	5.7	0.024	6.2×10^{-5}	0.031	8.0×10^{-5}	77
3.86	6.7×10^{-5}	18.5	8.2	0.080	2.1×10^{-4}	0.088	2.3×10^{-4}	90

[a] Three-layer PLGA−PAH−PSS-modified, negatively charged membrane, 33.2 cm^2 external area, 165 μm thickness. [b] Based on a 1:4 avidin:biotin binding ratio.

GOx (pI 4.7) and AP (pI 4.5) were immobilized on positively charged membranes at pH 6. The overall positive charge on the membrane was confirmed from Ca^{2+} rejection studies; on different membranes the rejection of 0.5 mM (20 mg/L) $CaCl_2$ varied from 50% to 70%.

Accessibility of the Active Sites. Biomolecules usually undergo conformational changes upon immobilization on solid supports; thus, an important factor is to establish the accessibility and orientation of the active sites. This was investigated using the well-known avidin−biotin interaction, which has been used by many researchers for site-specific enzyme immobilization[18,19] or recognition-based separations.[37,38] Avidin is a tetrameric protein, with four identical subunits, and each subunit can bind a biotin molecule.[39] Therefore, in the homogeneous phase 1 mol of avidin could bind maximally 4 mol of biotin. On the basis of this property, the objective was to establish whether the 4:1 biotin:avidin binding ratio changes after avidin immobilization. Avidin (pI 10.5) was immobilized on a three-layer negatively charged membrane (0.0166 mmol, as SO_3^-). To increase the immobilized amount, the pH was kept below the pI value, typically in a range from 6 to 8, so the protein has an overall positive charge. At this pH range, avidin has 18 positively and 12 negatively charged amino acid residues.[39] The amount of avidin immobilized on the two membranes is known, so this would correspond to 0.0010 and 0.0036 mmol of positive charge (NH_3^+), respectively. It can be observed that this is 1 order of magnitude lower than the negative charge on the membrane, so it can be assumed that all positive charge on avidin is neutralized. This is important since avidin immobilization was followed by the permeation of a biotinylated compound, BABA, which is negatively charged at the pH used. This fact further implies that charge interactions between the biotinylated compound and the immobilized avidin are unlikely to occur. The amount of BABA immobilized on the nylon−PLGA−PAH−PSS−avidin membrane was estimated from the material balance. On the basis of the above assumption, the amount of BABA immobilized was considered to be entirely due to avidin−biotin interaction. The nylon−PLGA−PAH−PSS membrane without avidin showed no BABA immobilization. Thus, the site binding accessibility on the two different membranes was found to be 77% and 90%, respectively (Table 4), suggesting that no major conformational changes occur due to protein−polyelectrolyte chain interactions. For comparison, in recent studies avidin was covalently (random) immobilized on the same type of membrane, and an accessibility of 50−55% was reported.[37,38] This demonstrates the superiority of electrostatic immobilization, as compared to random attachment of enzymes. Also, an additional benefit of electrostatic immobilization is membrane regeneration. After the membrane was washed with deionized water containing salt (NaCl, 0.5 M), 72% BABA was recovered. Further washing with deionized water at pH 11 ensures quantitative removal. The latter washing step also shows that a small amount of PSS chains (∼4%) were desorbed from the membrane.

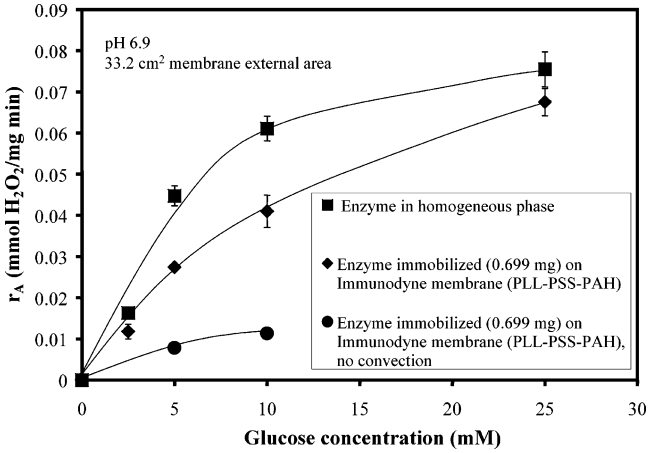

Figure 6. Initial rate of glucose oxidation measured by H_2O_2 formation at different substrate concentrations.

Enzymatic Catalysis. *Enzyme Activity*. Enzyme activities, in the free and immobilized forms, were evaluated using the classical Michaelis−Menten kinetics. The reaction rate can be expressed as

$$v = \frac{v_{max}[S]}{K_M + [S]} \tag{2}$$

where [S] is the substrate concentration, v_{max} is the maximum reaction rate attained at infinite substrate concentration, and K_M is the Michaelis constant.

Using the method of initial rates (initial slopes), the rate of product formation at several substrate concentrations was determined. Homogeneous-phase enzymatic reactions were carried out in a batch mode, and the initial rate was determined from the slope of product concentration vs time. For the immobilized enzyme, the feed solution containing the substrate was permeated through the membrane and permeate samples were collected at different times. The membrane was dried with nitrogen prior to the reaction being carried on to ensure that no water (which can dilute the permeate in the beginning of the reaction) is present beneath the membrane. The rate of product formation, r_p, was calculated as $r_p = \Delta C_p/m_{enz}\tau$, where C_p is the product concentration in the permeate, m_{enz} is the amount of the enzyme immobilized on the membrane, and τ is the residence time.

$\Delta C_p = C_p - C_{p,0}$ and $C_{p,0} = 0$, assuming that no product is formed outside the membrane. The polyelectrolyte chains and thus the enzymes are also immobilized on the membrane external area and at the pore mouth. This would result in product formation at the membrane feed side/solution interface. However, due to the fact that the operation occurs under convective flow conditions, we assumed that, once the product is formed at this interface, it will be transported through the membrane. That means the

(37) Hollman, A. M.; Christian, D. A.; Ray, P. D.; Galey, D.; Turchan, J.; Nath, A.; Bhattacharyya, D. *Biotechnol. Prog.* **2005**, *21*, 451−459.
(38) Datta, S.; Ray, P. D.; Nath, A.; Bhattacharyya, D. *J. Membr. Sci.* **2006**, ASAP article.
(39) Antisen, C. B.; Edsall, J. T.; Richards, F. M. In *Advances in Protein Chemistry*; Academic Press: New York, 1975; Vol. 29, p 85.

Table 5. Kinetics of Glucose Oxidase in Homogeneous-Phase and Immobilized Forms[a]

state of the enzyme	amt immobilized (μg)	K_m (mM)	V_{max} [(mmol/mg)/min]	rel activity (%)
homogeneous[b]	N/A	42.8 ± 3.4	0.313 ± 0.021	100
electrostatic immobilization[b]	249 ± 5	34.0 ± 2.9	0.204 ± 0.017	65
homogeneous[c]	N/A	33.3 ± 2.6	0.244 ± 0. 020	100
electrostatic immobilization[c]	699 ± 7	36.7 ± 2.4	0.189 ± 0.015	76
random immobilization[c]	55 ± 3	58.3 ± 4.6	0.006 ± 0.002	2

[a] Electrostatic immobilization on a PLL−PSS−PAH-modified, overall positively charged membrane, 33.2 cm^2 external area, 165 μm thickness. [b] Reaction carried out at pH 7.3. [c] Reaction carried out at pH 6.9.

Table 6. Kinetics of Alkaline Phosphatase (pI 4.5) in Homogeneous-Phase and Immobilized Forms[a]

state of the enzyme	amt immobilized (μg)	K_m (mM)	V_{max} [(μmol/mg)/min]	rel activity (%)
homogeneous	N/A	0.33 ± 0.07	26.2 ± 3.2	100
electrostatic[b] immobilization	138 ± 3	0.44 ± 0.12	18.5 ± 1.8	71
random immobilization	68 ± 6	0.67 ± 0.17	0.21 ± 0. 02	1
site-directed immobilization[c] (pH 8), ref 8	145 ± 12	0.255 ± 0.006	12.71 ± 0.8	85

[a] All experiments are at pH 6.5 unless noted. Substrate concentration 0.5−5 mM, four data points per experiment. [b] PLL−PSS−PAH, overall positively charged membrane, 33.2 cm^2 external area, 165 μm thickness. [c] On a protein A−antiFLAG−FLAG-modified MPS membrane, 17.3 cm^2 external area, 152 μm thickness.

product will not accumulate on the membrane's feed side. Although a quantitative relationship between the permeated flux and the product concentration at the membrane/feed side interface was not established, under our typical operating conditions, a flux of 15×10^{-4} $cm^3/(cm^2\ s)$ was maintained and no product was detectable in the feed solution. The permeated flux is inversely proportional to the residence time. On the basis of the previous assumption, the residence time in the membrane was calculated as $\tau = V/(AJ_v)$, where V is the membrane volume, A is the external area (33.2 cm^2), and J_v is the permeate flux. It should be noted that this permeation occurs through both the channel and the polyelectrolyte layer region, and thus, J_v includes an average flux for the entire region. Also, $V = \epsilon AL\phi$, where ϵ is the porosity (80% on average, from the manufacturer's data) and L is the membrane thickness (165 μm). ϕ is a correction coefficient for the membrane volume, with no immobilized enzyme, and it was estimated as explained below.

The enzyme is immobilized on the polyelectrolyte chains, extended from the pore wall toward the pore center, and thus, the chains do not cover the entire pore volume. The size of the pore volume (channel) unoccupied by the chains will have a significant effect on the kinetics. Substrate molecules can freely pass through the membrane without encountering the enzyme's active site. As a consequence, there will be no chemical reaction. The size of the channel (22% or 0.22 from the total pore volume) was estimated from permeability measurements for the bare and layered membrane. Thus, a correction coefficient of 0.78 was introduced into the calculation of the membrane volume to compensate for the fraction which contains no chains.

Equation 2 can be rearranged to

$$\frac{1}{v} = \frac{1}{v_{max}} + \frac{K_M}{v_{max}}\frac{1}{[S]} \qquad (3)$$

The kinetic parameters, maximum velocity, v_{max}, and apparent Michaelis constant, K_M, were determined from Lineweaver−Burk plots, $1/v$ vs [S], using linear regression, and the r^2 values were greater than 0.98.

A plot for the rates of hydrogen peroxide formation at four substrate (glucose) concentrations, with the enzyme in homogeneous and immobilized forms, is presented in Figure 6. The normalized activity for electrostaticaly immobilized enzyme approaches that of the homogeneous-phase value. It is important to note that, for the same membrane, the rate of product formation is increased 4-fold when operation occurs under convective flow conditions, as compared to soaking mode conditions. In the latter approach, the membrane is immersed in a beaker containing the glucose solution and O_2 is supplied. This clearly indicates that the enzyme is immobilized predominantly inside the pore and is not exposed on the membrane external surface and/or pore mouth. Otherwise, the rates of the product formation would be similar. Because the internal area is much larger than the external one, a much larger difference might be expected. It should be noted that the membrane has a large polydispersity, and the substrate is expected to diffuse inside the large pores even without convection, while smaller ones are less accessible. The convective flow increases the substrate transport through all membrane pores, making the immobilized enzyme more accessible and thus increasing the reaction rate.

The values for v_{max} and K_M for GOx and AP, in homogeneous and immobilized forms, are presented in Tables 5 and 6, respectively. It can be observed that apparent K_M values remain practically unchanged for both free and immobilized enzyme phases. K_M can increase considerably (2−10-fold),[13−15] due to partitioning of substrates between the solution and support and diffusional resistance to the transport of substrates to the enzymes. Thus, our data support the hypothesis that the operation under convective conditions can eliminate the diffusion-limited regime, the overall rate being limited by the turnover rate of the enzyme. Also, the relative activity for each enzyme immobilized electrostatically is much greater than that for random covalent immobilization.

As shown in Table 5, for GOx, the kinetic studies were conducted at two different amounts of GOx, immobilized on the membrane. The optimum enzyme loading is the highest amount that can be immobilized, without the activity being altered. Our data show that the optimum loading was not achieved, since with a 3-fold enzyme loading increase from 249 to 699 mg, the activity is increased from 65% to 76%, respectively. This implies that even if the normalized activity is practically unchanged (within error limits), the throughput increases linearly with the amount of enzyme immobilized. Also, it can be observed that the

maximum amount of GOx, covalently attached on the membrane, was 55 mg, which is 1 order of magnitude lower. The much lower enzyme loading can be explained by multiple-point enzyme−membrane binding, since there are 15 lysine residues per molecule of GOx, leading to the improper use of the active groups (suitable for amino covalent coupling) on the membrane.

In the case of electrostatically immobilized AP on the membrane, the relative activity was 71%. This value is close to the highest activity (85%), reported in the literature, for immobilized AP.[16] That particular approach in ref 16 involved site-directed attachment, obtained via protein fusion, which requires molecular biology techniques, a highly specific and complex methodology. The method presented in this work has the distinct advantage of simplicity, versatility, and potential regeneration. The high apparent relative activity, expressed as $v_{max,imm}/v_{max,hom}$, for both enzymes at different loadings, suggests that there is insignificant conformational change after enzyme immobilization in the pore assembly.

Enzyme Stability and Regeneration. The storage stability for GOx electrostatically immobilized on the multilayer assembly at 4 °C was tested over a period of time. Thus, after 8 days, the activity was still >94% of the original value (the activity right after immobilization). During this time, the enzyme was repeatedly used, showing that there is no enzyme leaching or deactivation during operation. For GOx stored in the homogeneous phase (nonmembrane case) at 4 °C, after 8 days, the activity was 69% compared to that of a fresh enzyme solution.

Both GOx (pI 4.7) and AP (pI 4.5) enzymes can be easily removed from the assembly, by permeating through the membrane DIUF water at pH 3.5. Bradford's assay analysis on the permeate solution confirmed quantitative removal of the enzyme from the membrane. In addition, after desorption from the membrane, for both enzymes, as expected, no product formation was detected when the substrate solution was permeated.

As mentioned previously, in the case of GOx, a control experiment using a single layer (PLL) for the electrostatic immobilization was conducted to check whether the three-layer assembly makes a significant difference. After GOx immobilization, under similar conditions, the amounts on the three-layer and single-layer assemblies were 699 and 490 μg, respectively. However, when the enzyme was immobilized on a single layer, after three washing steps with DIUF water at pH 5.8, 25% of the enzyme was desorbed. No enzyme desorption was detectable when washing was done with water under similar conditions. Moreover, when the enzyme was immobilized on a single layer, only after eight cycles did the rate of H_2O_2 formation decrease to 50%, as compared to the rate in the first cycle, and this was attributed to enzyme leaching during operation. For the case when the enzyme was immobilized on the three-layer assembly, there was a much better stability, as mentioned above. The multilayer assembly also offers more versatility, as the enzyme can be embedded within polyelectrolyte layers by alternate adsorption, which can significantly increase the stability within the structure. This was shown previously, on different supports.[24]

For AP, the enzyme activity after desorption (permeate) with DIUF water at pH 3.5 was tested compared to that of a fresh enzyme in the homogeneous phase. The pH of the wash solution containing the desorbed enzyme was adjusted from 3.5 to 6.5, and the substrate solution was added. Figure 7 shows the concentration of the product versus time profiles for both cases mentioned above. The amounts of enzyme were comparable (138 μg for the desorbed and 126 μg for the fresh solution).

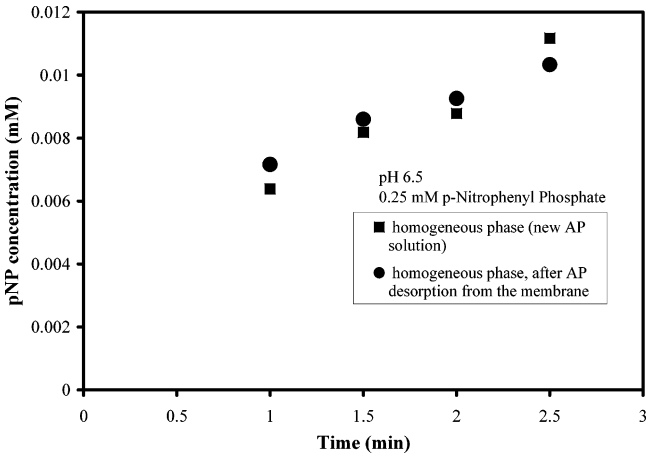

Figure 7. Alkaline phosphatase stability as measured by *p*-nitrophenol formation after desorption from the membrane.

Thus, after 6 days of repeated use, storage at room temperature, and desorption under acidic conditions, the rate from the slope of product formation is 67% as compared to that of a fresh enzyme solution. As a comparison, for an AP solution stored at room temperature for the same period of time, the enzyme retains only 25% of its original activity. After desorption from the assembly, a fresh AP solution was immobilized under similar conditions to check the regeneration capabilities. In this second step the amount immobilized was 113 μg, or 82%, as compared to that of the first step (138 μg).

Conclusions

Pore-assembled multilayers of polyelectrolytes have been successfully used for protein immobilization. Electrostatic immobilization is a simple and versatile method, as a variety of biomolecules can be incorporated into the polyelectrolyte multilayer assembly. Thus, the system can be used for affinity-based separations or as a membrane reactor, depending on the biomolecule incorporated. The overall charge on the protein and polyelectrolyte multilayers has a significant effect on the amount immobilized and system stability. The amount of protein immobilized on an oppositely charged membrane under convective flow is 25-fold higher than for the case when both the membrane and protein have similar charges. High active site accessibility after immobilization, confirmed by affinity interaction (avidin−biotin) and two enzymatic reactions (catalyzed by GOx and AP), suggests that only minor conformational changes occur after biomolecule immobilization. Also, reusability and the ease of regeneration constitute additional advantages of this technique. Moreover, the proper choice of membrane support, pore size, nature of the polyelectrolytes (weak or strong), chain length, and operational parameters (membrane flux, pH, temperature, ionic strength) can further increase the overall effectiveness of this method.

Acknowledgment. This work was supported by the NIEHS-SBRP program and by the University of Kentucky Center of Membrane Sciences.

Supporting Information Available: Details about the experiments, polyelectrolyte, protein immobilization, active site accessibility determination, and enzyme kinetics. This material is available free of charge via the Internet at http://pubs.acs.org.

LA061124D